AN ELECTRICALLY-CONTROLLED AXIAL-FLUX PERMANENT MAGNET GENERATOR

Piotr Paplicki, Pawel Prajzendanc, Marcin Wardach

West Pomeranian University of Technology in Szczecin, Faculty of Electrical Engineering, Department of Power Systems and Electrical Drives, Szczecin, Poland

Abstract. The paper presents a design of an axial-flux surface-mounted permanent-magnet generator with flux-regulation capability. Based on three-dimensional finite-element analysis (3D-FEA), the no-load air-gap magnetic flux density, flux-control characteristics, cogging torque and electromagnetic torque of the machine have been predicted. Simulation results of no-load back-EMF waveforms performed at different DC control coil excitations have been compared with experimental results.

Keywords: axial-flux machine, PM generator, hybrid excitation, flux-control, voltage regulation

GENERATOR TARCZOWY Z MAGNESAMI TRWAŁYMI Z ELEKTRYCZNIE KONTROLOWANYM WZBUDZENIEM

Streszczenie. W artykule przedstawiono projekt generatora tarczowego z powierzchniowo mocowanymi magnesami trwałymi z możliwością regulacji strumienia wzbudzenia. Na podstawie trójwymiarowej analizy polowej metodą elementów skończonych (3D-MES) wyznaczono rozkład indukcji magnetycznej w szczelinie powietrznej, charakterystykę regulacji strumienia, moment zaczepowy oraz moment elektromagnetyczny maszyny. Symulowany przebieg napięcia indukowanego w uzwojeniach stojana w funkcji prądu DC dodatkowego uzwojenia wzbudzeniu maszyny porównano z wynikami eksperymentalnymi.

Słowa kluczowe: maszyna tarczowa, generator z magnesami trwałymi, wzbudzenie hybrydowe, regulacja strumienia, regulacja napięcia

Introduction

Nowadays, development in the field of unconventional permanent magnet (PM) synchronous generators with adjustable flux capabilities is clearly observed. They can effectively regulate terminal voltage with an inverter control technique or a hybrid-excitation technique with a flux-control (FC) capability, and they can be used in propulsion applications with frequent rotational speed variations such as generators in small wind turbines mounted at low altitudes.

In order to control the air-gap flux of a PM machine successfully, many different novel machine concepts have been recently designed [1–7, 9, 11–15]. This increased attention is mainly due to their wide speed-control range with flux-weakening (FW) or field-strengthening (FS) operation.

It should be noted that although PM machines have limits, e.g the risk of demagnetization of the PMs, they are still the most used type of machines in variable speed drive applications. Ensuring the effective air-gap flux control of the machine in FW operation is also a challenge.

The paper shows a design and the preliminary results of a Field-controlled Axial-flux PM machine (FCAFPM-machine) with the FC feature. A field control range (FCR) factor was introduced and used in the study as a measure of the effectiveness of the machine flux control. The FCR factor is calculated as the ratio of the linked flux Ψ_s of the machine, taken from the FS operation, occurring under a positive DC control coil current (I_{DC+}), to the FW operation, arising under the negative value of the DC control coil current (I_{DC-}).

1. Structure of FCAFPM-machine design

1.1. FCAFPM-machine topology description

The base model of the FCAFPM machine is a PM axial flux machine consisting of an inner double-wound stator and two outer rotors. Additional elements of the FCAFPM are a metal bushing (7) connecting the rotors and an additional DC control coil (5) fitted inside the stator, as shown in Figure 1. It should be pointed out that the presented machine design has been previously investigated and partially described in [8, 10].

The stator of the FCAFPM machine can be made of one or two toroidal cores (1), around which the phase windings (6) are wound. An additional DC coil (5) with 500 turns is mounted on the inner surface of the stator. The coil resistance is 4.8 Ω. The DC coil, as an additional excitation of the constant field

together with the stator, is stationary, thanks to which there are no brushes and slip rings for it. The rotor's magnetic circuit consists of two disc yokes (2) and a connecting metal bushing (7). Six iron (4) and PM (3) poles are mounted alternately facing each other on each disc. All magnets are axially polarized in the same direction. The rotor disks (yokes), iron poles (IP) and the bushing are made of magnetic steel and rotate on a non-magnetic shaft (8).
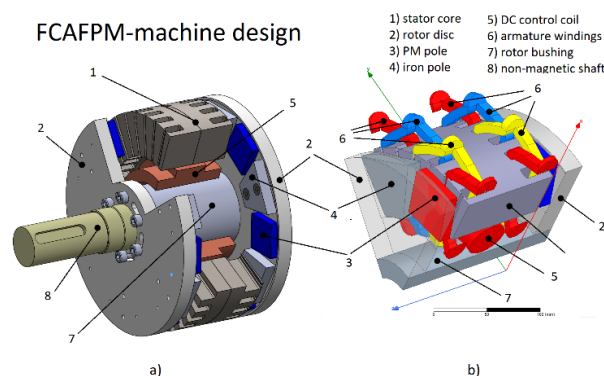

Fig. 1. Structural model (a) and 3D fine element method (FEM) model (b) of FCAFPM-machine

The selected dimensions of the proposed machine are listed in Table 1. Each disc has 6 pairs of poles, which gives a total of 12 pairs of poles. The machine does not have additional cooling, so it was assumed that the current density in the stator and DC coil windings would not exceed 5 A/mm^2. It should be noted that the presented machine design is not optimized yet, and is intended for low speed generator design.

Table 1. Dimensions of proposed FCAFPM-machine

Parameters	value
External radius of the stator	300 mm
Internal radius of the stator	180 mm
Thickness of the stator	100 mm
Number of stator slots	36 (double sided)
Axial length of the rotor disk	20 mm
Thickness of the IP	15 mm
Dimensions of the PM	50x50x12 mm
Height of the air gap above the IP	1 mm
External radius of the rotor bushing	50 mm

1.2. FCAFPM-machine prototype

Figure 2a shows a FCAFPM-machine prototype which has been developed and assembled for validation purposes. Figure 2b shows the stator and rotor components before machine assembly, where the PMs are protected against mechanical damage and centrifugal forces with special 3D-printed shields. The DC control coil is located between the front terminals of the stator coils and is sealed with epoxy resin.
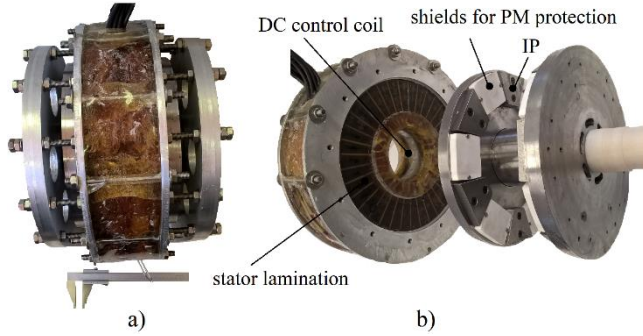

Fig. 2. FCAFPM-machine prototype (a) and stator and rotor components before assembly (b)

Figure 3 shows the manufactured rotor disc with IPs already mounted, along with its main dimensions. The IP base has the shape of an isosceles trapezoid with arms inclined to each other at an angle of 45°. This IP shape was used to reduce the cogging torque of the PM machines. The primary excitation field of the generator is from the cuboid-shaped PMs that are mounted between the IPs. The PMs are made of N-38SH material with the following basic parameters: remanence = 1.23 T, coercivity = 907 kA/m at 20°C, and $(BH)_{max} \approx 300$ kJ/m³. Both the IPs and PMs are mounted on the rotor in a special groove with a depth of 1 mm. The IPs are bolted to the rotor yoke with screws, while the PMs are glued and surrounded by a 3D-printed shield. The thickness of each PM is 12 mm and the thickness of each IP is 15 mm, which results in an air gap above the magnets of 4 mm, and over IPs of 1 mm.
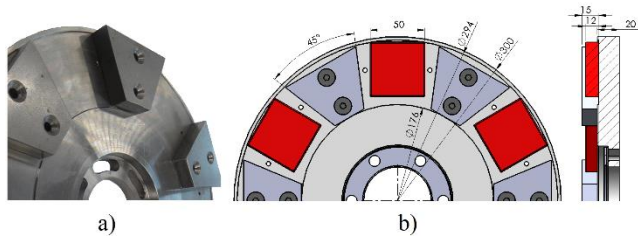

Fig. 3. Design of disc type rotor yoke with IPs

2. Results of FEM simulation and experimental tests

This part of the article presents the 3D-FEA results including magnetic flux density distribution, air-gap flux density, no-load flux linkage, cogging torque, phase winding back-EMF waveforms, and experimental validation.

2.1. Magnetic field test results

The magnetic flux from the PMs and the additional constant magnetic field generated by the DC coil current (I_{DC}) together constitute the total flux of the machine Φ_{tot}. Air-gap flux regulation is achieved by increasing the current I_{DC}. In other words, magnetic flux generated by the DC excitation windings Φ_{DC} interacts with the magnetic flux excited by the PMs (Φ_{PM}). In the FW operation, the magnetic flux produced by the DC excitation coil reduces the total air-gap flux. When the DC current reverses its direction, the total air-gap flux is increased.

This relation can be express by the following equations:

$$\phi_{tot} = \phi_{tot/PM} + \phi_{tot/DC} \tag{1}$$

$$\phi_{tot/PM} = \phi_{PM/PM} + \phi_{IP/PM} \tag{2}$$

$$\phi_{tot/DC} = \phi_{PM/DC} + \phi_{IP/DC} \tag{3}$$

where: ϕ_{tot} – total air-gap flux; $\phi_{tot/PM}$ – air-gap flux component created by a PM over one pole; $\phi_{tot/DC}$ – air-gap flux component created by the DC excitation field over one pole; $\phi_{PM/PM}$ – air-gap flux component created by a PM in front of the PM pole; $\phi_{IP/PM}$ – air-gap flux component created by a PM in front of the IP; $\phi_{PM/DC}$ – air-gap flux component created by the DC excitation field in front of the PM pole; and $\phi_{IP/DC}$ – air-gap flux component created by the DC excitation field in front of the IP.

In order to evaluate the performance and air-gap flux control of the machine concept, a simulation study was carried out. The simulation study was performed by using 3D finite element analysis (3D-FEA) at various levels of magnetomotive force (MMF) excited by the DC control coil. In this study, the MMF, expressed as ampere-turns (AT), is defined as the product of the DC control coil current I_{DC} and the number of turns of the coil.

Figure 4 shows the no-load magnetic flux density distribution on the rotor and stator cores of the machine (left) and the magnetic flux density in the middle of the air-gap (right). The 3D-FEA model of the FCAFPM machine was developed in the ANSYS software package and was limited to one sixth of the whole machine.

Figure 5 shows the air-gap flux distribution under three different MMFs, for comparison, meaning under no-load ($I_{DC} = 0$) and $I_{DC} = \pm5A$ (MMF ±2500 AT) loading conditions.
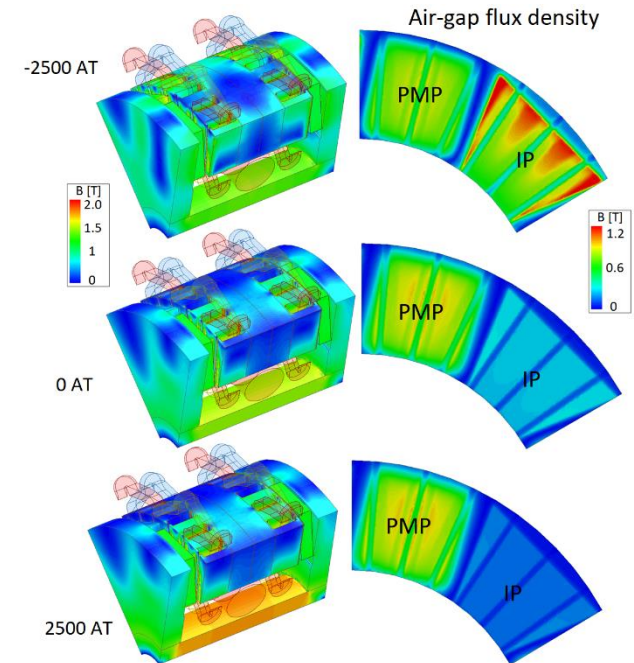

Fig. 4. Magnetic field distribution in the machine (left) and the two-dimensional air-gap flux density distribution over one pole pair under different MMF excitations – 0 and ±2500 AT (right).

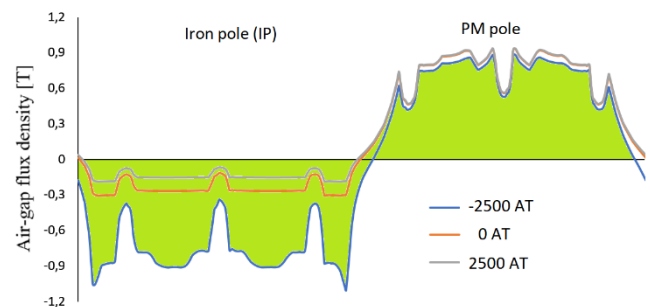*Fig. 5. Air-gap flux density distribution over one pole pair under different MMF excitations – 0 and ±2500 AT*

In order to predict the no-load FC characteristics of the machine, 3D-FEA investigations were carried out.

Figure 6 shows phase magnetic flux linkage waveforms produced by the rotor permanent magnets, and the DC excitation field for three different MMFs.

The results in Figures 4 and 5 show that the MMF generated by the DC in the extra coil changes the air-gap flux distribution, and consequently, the stator flux linkage (Ψ_s) is effectively changed. The result can be seen in Figure 6, where the maximum values of flux linkage Ψ_{sm} under different MMF excitation levels operations are changed (under FS-operation, it is 780 mWb, no-load = 232 mWb, and FW-operation = 114 mWb). The results confirmed that controlling the DC field excitation successfully changes the stator flux linkage. The results also show that the FW operation is less effective than the FS operation, under the same MMF condition.
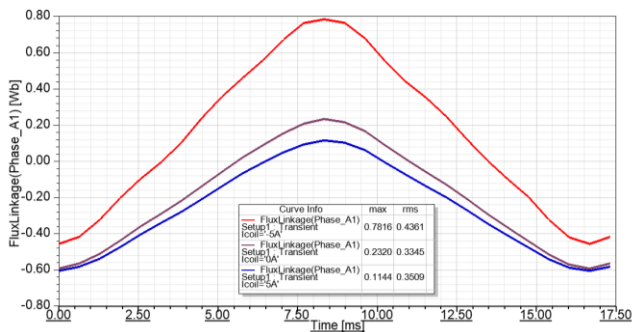

Fig. 6. 3D-FEA effect of no-load stator flux linkage (Ψ_s) waveforms at different MMF excitation levels

2.2. Electromagnetic torque test results

Low torque ripple is mostly required in generators to reduce acoustic noise and mechanical vibration. The effect of the shapes of the IP and PM poles on the cogging torque of the machine was investigated by a 3D-FEA time-stepping analysis.

The cogging torque simulation results are shown in Figure 7, where it can be seen that the maximum value of cogging torque is approximately 2.2 Nm, and this is observed during FS operation. During FW operation, the cogging torque waveform is slightly different from the waveform obtained under the no-load DC excitation field.
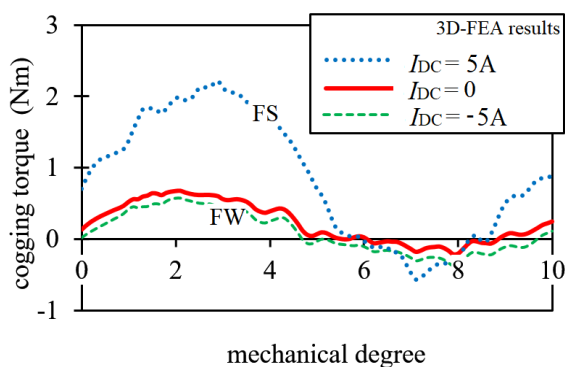

Fig. 7. 3D-FEA predictions of cogging torque waveforms at three different values of DC control coil current

The results show that the maximum value of cogging torque is significantly increasing during FS operation, and it should be reduced, e.g. by considering the skewed stator or rotor method.

In order to analyse the influence of the DC excitation field on the optimum current phase angle for the purposes of maximum torque determination, the electromagnetic torque versus angle rotor position characteristics were calculated and are shown in Figure 8. The electromagnetic torque waveforms including cogging torque were analysed for three different MMF conditions and at a constant DC armature current (I_s) of 100 A for phase A and 50 A for phases B and C.
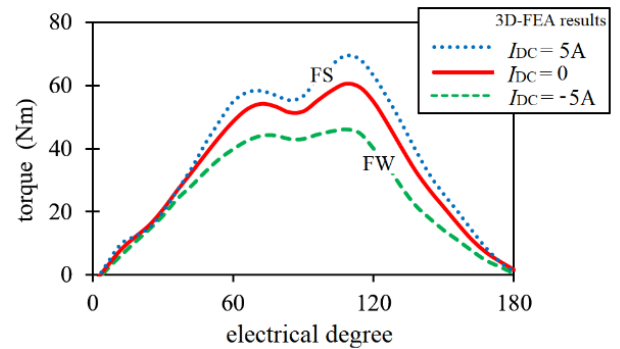

Fig. 8. 3D-FEA results of torque angle characteristics at three different values of the DC control coil currents

The maximum steady torque of the machine is 69.3 Nm (for FS operation), 60.4 Nm (no-load MMF) and 46.0 Nm (for FW operation).

3. Experimental validation

This section compares the simulation and experimental results of the back-EMF waveforms obtained under three different MMFs.

3.1. Experimental setup

To verify the FCR of the machine, an experimental setup for the proposed FCAFPM-machine as a generator was built and is shown in Figure 9. The machine prototype is mechanically connected to a 10-kW PMSM machine. In order to control current I_{DC} of the DC control coil, a controllable AC/DC power supply unit was used.
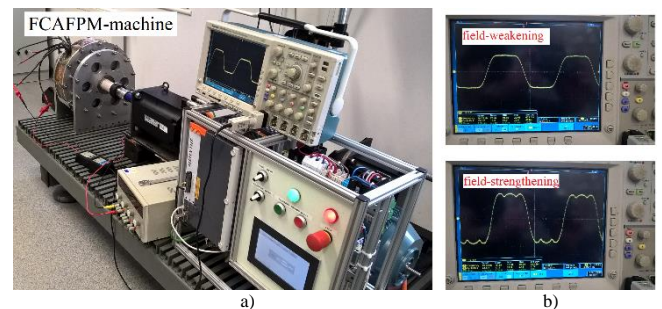

Fig. 9. Experimental setup (a) and oscilloscope screen showing back-EMF waveforms (b) for the FCAFPM-machine at a rotor speed of 200 rpm measured at two MMF excitations under FW (upper) and FS operation

3.2. No-load back-EMF control validation

No-load tests were performed using the PMSM drive machine. The tests were carried out at a rotor speed of 200 rpm, under different DC excitation fields, where the current I_{DC} was varied between positive and negative values. Figure 9 shows the terminal voltage achieved at two different MMF excitation levels of ±2500 AT. As seen on the oscilloscope screen, the root-mean-square (RMS) value of the terminal voltage increased from 15.0 V to 22.5 V as the excitation of the MMF increased from 0 AT to 2500 AT (by I_{DC} = ±5.0 A).

It can be seen that the FW operation does not affect the induced voltage waveform, which is trapezoidal. On the other hand, the field amplification operation caused the appearance of additional harmonics that distorted this waveform. Optimizing the geometry of the IPs can reduce or even eliminate this problem.

Figure 10 compares the no-load terminal voltage and the simulation of back-EMF. As can be seen in the figure, the measured results match the 3D-FEA predictions well.
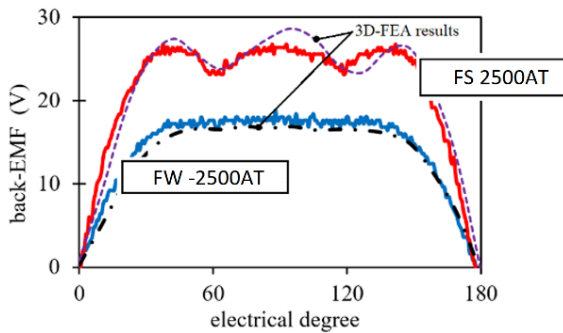
Fig. 10. Comparison of simulation and experimental results of no-load back-EMF waveforms of the FCAFPM-machine at a rotor speed of n = 200 rpm, at three different MMF excitation levels

Table 2 shows the effective values of the electromotive force induced in the stator windings at a rotor speed of 200 rpm for different magnetomotive forces in the DC coil. It can be seen that the results for both MMF = -2500 AT and MMF = 2500 AT are very similar, which confirms the correctness of the theoretical assumptions and the models.

Table 2. Phase-induced voltage

	Simulation	Experiment
MMF = 2500 AT	14.6 V	15.0 V
MMF = 0 AT	16.0 V	16.2 V
MMF = -2500 AT	23.5 V	22.5 V

4. Conclusion

Both the simulation and experimental results confirm that the FCAFPM-machine design concept can be effectively used as a generator with regulated output voltage.

Moreover, the developed FCAFPM-machine concept with air-gap flux boosting capability has an important feature that allows the control of the power energy for several electric machines and applications, for example in electric vehicles, where constant power operation across a wide range of speeds is required. In the same way, the output power of a wind turbine varies in a way which is highly correlated to wind speed. It is a challenging task to generate the required output power regardless of the wind conditions, within a certain range of wind speeds.

The presented machine prototype can be used as a low-speed 3 kW power generator with hybrid excitation to overcome the variation of output power on wind speed in the range of 50%.

The full experimental results for both load and fault conditions will be presented in future papers.

References

[1] Afinowi I. A. A., et al.: Hybrid-Excited Doubly Salient Synchronous Machine With Permanent Magnets Between Adjacent Salient Stator Poles. IEEE Transactions on Magnetics 51(10), 2015, 8107909, 1–9 [https://doi.org/10.1109/TMAG.2015.2446951].

[2] Aydin E., et al.: A hybrid-excited axial transverse flux permanent magnet generator. IEEE Energy Conversion Congress and Exposition (ECCE) – Milwaukee, 2016, 1–6 [https://doi.org/10.1109/ECCE.2016.7854701].

[3] Aydin M., Surong H., Lipo T.A.: Design, Analysis, and Control of a Hybrid Field-Controlled Axial-Flux Permanent-Magnet Motor. IEEE Transactions on Industrial Electronics 57(1), 2010, 78–87 [https://doi.org/10.1109/TIE.2009.2028294].

[4] Di Barba P., et al.: Hybrid excited synchronous machine with flux control possibility. International Journal of Applied Electromagnetics and Mechanics 52(3-4), 2016, 1615–1622 [https://doi.org/10.3233/JAE-162190].

[5] Dupas A., et al.: Investigation of a New Topology of Hybrid-Excited Flux-Switching Machine With Static Global Winding: Experiments and Modeling. IEEE Transactions on Industry Applications 52(2), 2016, 1413–1421 [https://doi.org/10.1109/TIA.2015.2497305].

[6] Hua H., Zhu Z. Q., Zhan H.: Novel Consequent-Pole Hybrid Excited Machine With Separated Excitation Stator. IEEE Transactions on Industrial Electronics 63(8), 2016, 4718–4728 [https://doi.org/10.1109/TIE.2016.2559447].

[7] Lee C. H. T., Liu C., Chau K. T.: A magnetless axial-flux machine for range-extended electric vehicle. Energies 7(3), 2014, 1483–1499, https://doi.org/10.3390/en7031483].

[8] Paplicki P., Prajzendanc P.: The Influence of Permanent Magnet Length and Magnet Type on Flux-control of Axial Flux Hybrid Excited Electrical Machine. 14th Selected Issues of Electrical Engineering and Electronics (WZEE), 2018 [https://doi.org/10.1109/WZEE.2018.8749015].

[9] Paplicki P.: A novel rotor design for a hybrid excited synchronous machine, Archives of Electrical Engineering 66(1), 2017, 29–40 [https://doi.org/10.1515/aee-2017-0003].

[10] Paplicki P.: Modified concept of axial-flux permanent magnet machine with field weakening capability. Archives of Electrical Engineering 63(2), 2014, 177–185 [https://doi.org/10.2478/aee-2014-0014].

[11] Tapia, J. A., Leonardi, F., Lipo, T. A.: Consequent-Pole Permanent-Magnet Machine with Extended Field-Weakening Capability. IEEE Transactions on Industry Applications 39(6), 2003, 1704–1709 [https://doi.org/10.1109/TIA.2003.818993].

[12] Wang Q., Niu S., Luo X.: A Novel Hybrid Dual-PM Machine Excited by AC With DC Bias for Electric Vehicle Propulsion. IEEE Transactions on Industrial Electronics 64(9), 2017, 6908–6919 [https://doi.org/10.1109/TIE.2017.2682778].

[13] Wardach M., et al.: Novel Hybrid Excited Machine with Flux Barriers in Rotor Structure. COMPEL – The international journal for computation and mathematics in electrical and electronic engineering 37(4), 2018, 1489–1499 [https://doi.org/10.1108/COMPEL-08-2017-0364].

[14] Wardach M., Paplicki P., Palka R.: A hybrid Excited Machine with Flux Barriers and Magnetic Bridges. Energies 11, 2018, 676 [https://doi.org/10.3390/en11030676].

[15] Zepp L. P., Medlin J. W.: Brushless permanent magnet motor or alternator with variable axial rotor/stator alignment to increase speed capability. US 6555941 B1, 2003.

D.Sc. Ph.D. Eng. Piotr Paplicki
e-mail: piotr.paplicki@zut.edu.pl

Piotr Paplicki was born in Pyrzyce, Poland in 1975. Graduated and received a Ph.D. degree from the Electrical Department, Szczecin University of Technology, Szczecin, Poland, in 2001 and 2006, respectively. Since 2017, he has been an Associate Professor with the Faculty of Electrical Engineering, West Pomeranian University of Technology, Szczecin, Poland. From 2016 until now, Vice-Dean for Student Affairs. His research interests include the design of electrical machines and drives.

http://orcid.org/0000-0003-0364-2028

M.Sc. Eng. Pawel Prajzendanc
e-mail: pawel.prajzendanc@zut.edu.pl

Pawel Prajzendanc was born in Pyrzyce, Poland in 1990. Received a B.S. degree in electrical engineering from West Pomeranian University of Technology, Szczecin, Poland in 2015 and an M.S. degree in 2017. He is currently pursuing a Ph.D. degree in electrical engineering at the Faculty of Electrical Engineering, West Pomeranian University of Technology, Szczecin, Poland. His awards and honors include a scholarship of Prime Minister of Poland. His research interests include the design of electrical machines and drives.

http://orcid.org/0000-0002-1662-4390

D.Sc. Ph.D. Eng. Marcin Wardach
e-mail: marcin.wardach@zut.edu.pl

Marcin Wardach was born in Barlinek, Poland in 1980. He graduated and received a Ph.D. degree from the Electrical Department, Szczecin University of Technology, Szczecin, Poland, in 2006 and 2011, respectively. From 2020 until now, he has been an Associate Professor with the Faculty of Electrical Engineering, West Pomeranian University of Technology, Szczecin. His research interests include the design of electrical machines and drives.

http://orcid.org/0000-0002-1017-9054